ELSEVIER

Catalysis Today 78 (2003) 171–180

CATALYSIS TODAY

www.elsevier.com/locate/cattod

Characterisation of alumina-supported vanadium oxide catalysts by kinetic analysis of H_2-TPR data

Jaana M. Kanervo [a,*], M. Elina Harlin [b], A. Outi I. Krause [a], Miguel A. Bañares [c]

[a] *Department of Chemical Technology, Helsinki University of Technology, P.O. Box 6100, FIN-02015 HUT, Finland*
[b] *Fortum Oil and Gas Oy, Research and Technology, P.O. Box 310, FIN-06101 Porvoo, Finland*
[c] *Institute of Catalysis and Petroleum Chemistry, CSIC, Campus Cantoblanco, E-28049 Madrid, Spain*

Abstract

Alumina-supported vanadium oxide catalysts with vanadium contents of 2, 5 and 11 wt.% were prepared by incipient wetness impregnation and characterised by XRD, Raman spectroscopy and H_2-TPR. The catalysts with the low vanadium contents contained vanadium mainly in the well-dispersed phase, but the catalyst with the highest vanadium content contained also some crystalline $AlVO_4$ according to XRD and Raman spectroscopic results. The reduction kinetics of the vanadium catalysts was modelled based on the hydrogen consumption during the TPR. The reduction kinetics could be described with a single-reducible-site random nucleation model for the catalyst containing the lowest amount of vanadium. The reduction kinetic models for the other catalysts required a combination of multiple processes to describe the experiments properly. In the catalyst with 5 wt.% V, a part of vanadium species possibly reduces as a homogeneous random nucleation process, but topochemical reduction by nuclei growth also takes place. In the catalyst with 11 wt.% V, reduction by nuclei growth seems to be the predominant reduction mechanism. The characterisation of the reduced catalysts by XRD and during reduction by Raman spectroscopy enabled the identification of the features of the TPR profiles.

Keywords: Vanadia catalysts; Reduction kinetics; Raman spectroscopy

1. Introduction

Supported vanadium oxides selectively catalyse many reactions such as partial oxidation of hydrocarbons, oxidative dehydrogenation of alkanes and selective reduction of NO_x [1–5]. The redox properties of the catalyst are important for reactions, which proceed via the Mars-van Krevelen mechanism [6]. Hydrocarbon molecules react with oxygen atoms and the reduced vanadium cations that are formed are reoxidised in the oxidative atmosphere. The average oxidation state during catalytic operation depends on the relative rates of reduction and reoxidation, which for supported vanadium oxide catalysts appears to leave the supported oxide essentially oxidised [7,8].

In oxidative dehydrogenation of alkanes, the reducibility of vanadium species has been related to the activity and selectivity of the catalyst [9–11]. Understanding of the reduction behaviour is therefore essential for the development of the catalysts for these reactions. Temperature-programmed reduction (TPR) is a very convenient technique for studying the reduction behaviour of supported oxide catalysts qualitatively. Furthermore, TPR provides detailed information regarding reduction kinetics. Reducibility investigations by temperature-programmed or isother-

* Corresponding author. Fax: +358-9-451-2622.
E-mail address: kanervo@polte.hut.fi (J.M. Kanervo).

0920-5861/02/$ – see front matter
PII: S0920-5861(02)00326-7

mal studies on vanadium oxide catalysts have been reported in numerous papers. The kinetics of reduction of these oxides has been evaluated in a few publications [9,12–15,24–26]. In this investigation we extend the knowledge regarding the reduction behaviour of supported vanadium oxide catalysts [16,17] by using similar kinetic analysis methodology we previously applied for the TPR of supported chromium oxide catalysts [18,19]. Kinetic models for gas–solid reactions are now tested against experimental H_2-TPR data of three vanadium oxide catalysts with different vanadium loading. Kinetic parameters are estimated using nonlinear regression analysis. To further assess the nature of reducing vanadium species, the catalysts are characterised by XRD and Raman spectroscopy.

2. Experimental

2.1. Catalyst preparation

Supported vanadium oxide catalysts were prepared by the incipient wetness impregnation method with alumina as the support. Before impregnation, the alumina support (Akzo Nobel 000-1.5E) was crushed and sieved to a particle size of 0.3–0.5 mm and calcined at 750 °C for 16 h with 5% oxygen in nitrogen (Aga, O_2 99.998%, N_2 99.999%). The impregnation was accomplished by dissolving NH_4VO_3 (Merck, >99%) in an aqueous solution of oxalic acid (Riedel-de Haën AG, >99.5%). After impregnation the catalyst was dried at 120 °C for 8 h and calcined at 700 °C for 2 h.

2.2. Catalyst characterisation

The amount of vanadium in the catalyst was measured by atomic absorption spectroscopy (AAS). The surface area of the catalyst was determined with a Coulter Omnisorp 100CX (static volumetric method).

The H_2-TPR measurements were performed with an Altamira Instruments AMI-100 catalyst characterisation system. The catalyst samples (50 mg) were dried at 130 °C for 60 min in argon, calcined at 600 °C for 30 min and cooled down to 30 °C under 5% O_2/He. TPR was performed at heating rates of 6, 11, 17 °C/min up to 630 °C under a flow of 10.7% H_2/Ar (30 cm^3/min). The consumption of hydrogen was monitored with a thermal conductivity detector (TCD) and recorded at a signal rate of 6 points/min. The hydrogen consumption was quantified by a pulse calibration. The temperature was measured adjacent to the catalyst bed and it followed a strictly linear trend during the TPR. The selection of experimental conditions for TPR was in agreement with the criterion developed by Malet and Caballero [20], $P = \beta S_0/(FC_0) \ll 20\,\mathrm{K}$ (β is the heating rate, S_0 the initial molar amount of reducible substance, F the volumetric flow rate of reducing agent and C_0 the molar concentration of reducing agent). The instantaneous maximum conversion of hydrogen was less than 4% in our system: no hydrogen exhaustion took place. The experimental set-up allowed treating the system as a differential reactor. The effect of diffusion of hydrogen in the catalyst pores was considered in terms of the Weisz-Prater [21] criterion. The value of the criterion $\ll 1$ indicated that the observed reaction rate was free of the intraparticle mass transfer resistance of the reactant.

The crystalline structure of the calcined and reduced catalysts was studied by X-ray diffraction (XRD) analysis with a Siemens D500 instrument using Cu Kα radiation. The catalysts were dried and calcined as described above. The catalysts were then reduced with 10% H_2/Ar (30 cm^3/min) to 480 or to 650 °C with 10 °C/min. After that the sample was inertly transferred to the XRD instrument and analysed under N_2 atmosphere, in a special sample holder equipped with a half-cylindrical Mylar window. Moreover, the sample was again reoxidised at 600 °C in 5% O_2/He and analysed by XRD.

Raman spectra during TPR (TPR-Raman) experiments were run with a hot stage (Linkam TS-1500) that can be heated up to 1500 °C under flowing gases. The hot stage was attached to a Renishaw System-1000 microscope Raman spectrometer with an Ar^+ laser as exciting source at 514 nm. TPR-Raman experiments were run by heating the sample from 300 to 795 °C in steps of 33 °C. Spectra were acquired at each temperature, with a resolution of 2 cm^{-1}. Laser power was 12 mW and acquisition time was selected to be 5, 2 and 1 min, depending on the vanadium oxide loading that increases the signal-to-noise ratio. 1% H_2 in Ar (SEO-L'Air Liquide) was used for

the TPR-Raman experiments. Selected spectra are presented to illustrate the trends.

2.3. Estimation of kinetic parameters

Kinetic parameters were estimated by non-linear regression. The integral was numerically solved by either a trapezoidal method or an adaptive Simpson quadrature, and the object function minimisation was carried out by the Nelder-Mead search method. The criterion for optimisation was the sum of squared residuals (SSRs) between the measured hydrogen consumption and the corresponding model solution. In the multi-response fitting, a combined criterion was formed by adding up the SSRs. All the computations were performed in the MATLAB®6 (MathWorks Inc.) environment. The temperature mean-centering was done for the rate coefficients $k(T) = k_{\mathrm{ref}} \exp(E/R(1/T_{\mathrm{ref}} - 1/T))$ in order to enhance parameter identifiability. T_{ref} was set as 750 K.

3. Results

3.1. The catalyst

The vanadium contents of the catalysts were 2.0, 5.2 and 11.4 wt.%. The catalysts were designated according to the measured amount of vanadium V2, V5 and V11, respectively. The surface area of the alumina support was 181 m^2/g after calcination at 750 °C.

The XRD diagrams of the catalysts are shown in Fig. 1. The XRD patterns for the V2 and V5 catalysts were similar to the one for the alumina support, whose XRD pattern included possibly both γ- and δ-alumina after calcination at 750 °C. The vanadium oxide was, thus, well dispersed on the surface of the support with the crystalline size below the detection limit of the method. The XRD pattern for V11 indicated, however, the presence of crystalline $AlVO_4$. In addition, the crystalline size of the alumina was increased with vanadium addition.

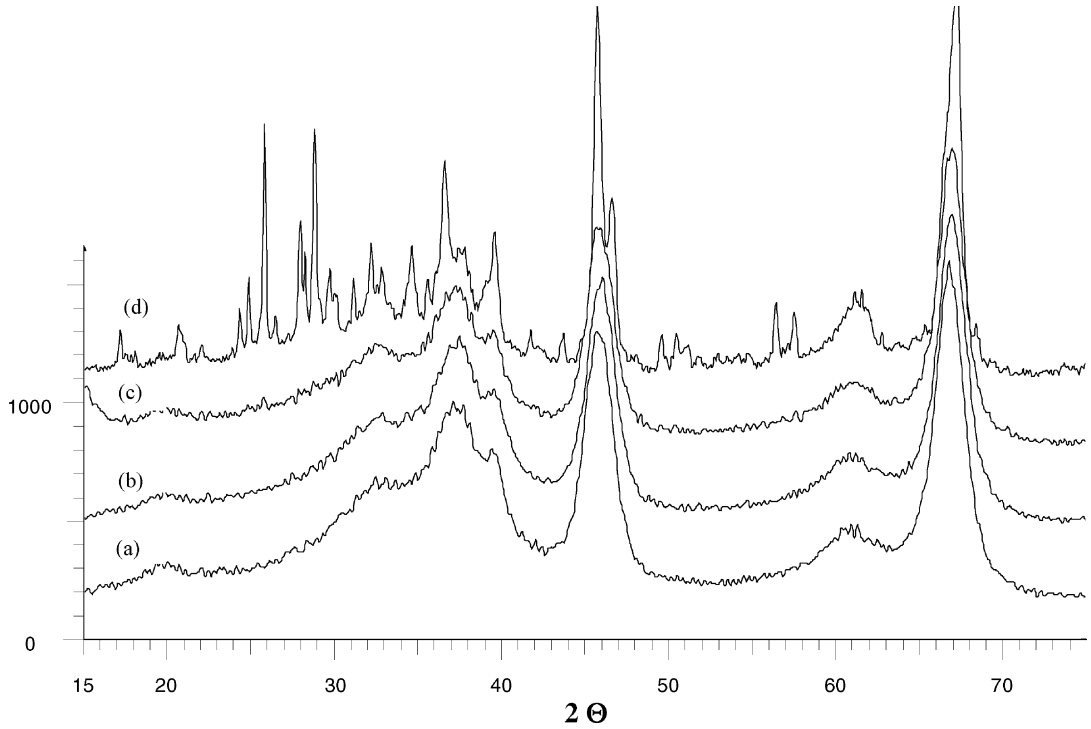

Fig. 1. XRD patterns of (a) alumina after calcination at 750 °C, (b) V2, (c) V5 and (d) V11.

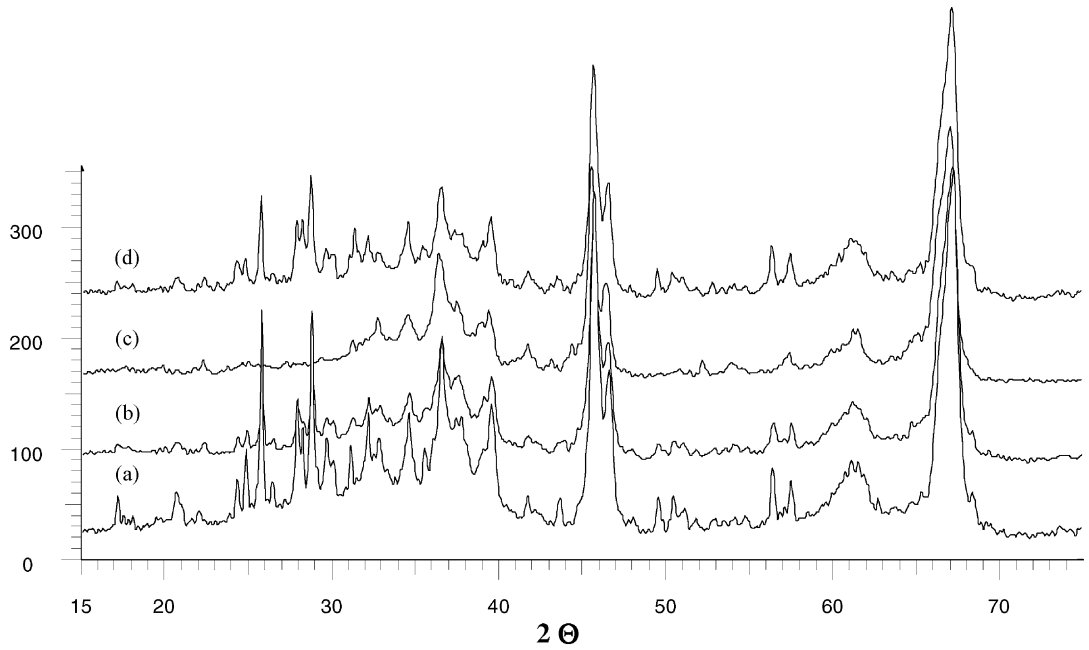

Fig. 2. The XRD patterns of V11 (a) as such, (b) after reduction to 480 °C, (c) after reduction to 650 °C and (d) after oxidation at 600 °C.

The XRD analysis was also performed with V11 samples reduced to 480 or to 650 °C (Fig. 2). The pattern after reduction to 480 °C was similar to the one for the oxidised catalyst. However, the peaks for the crystalline $AlVO_4$ disappeared after reduction to 650 °C and appeared again after the following oxidation. The crystalline $AlVO_4$ was thus reduced at temperatures between 480 and 650 °C.

The Raman diagrams for hydrated and dehydrated samples are presented in Fig. 3. The Raman results indicate that there are surface vanadium oxide species on fresh V2 and V5, whereas V11 show intense Raman bands for $AlVO_4$ at 1003, 970, 943, 913, 882, 515, 399, 320, 290, 282 cm^{-1}. In TPR-Raman data for V2 and V5, the disappearance of vanadium oxide bands (V=O 1020 cm^{-1}, V–O–V near 900 cm^{-1}) confirms that there are both isolated and polymeric surface vanadium oxide species. Isolated vanadium oxide species on the surface have one terminal V=O bond (1020 cm^{-1}) and three V–O–Al bonds that are not active in Raman. Surface polymeric vanadium oxide species possess one terminal V=O bond (1020 cm^{-1}) and bridging V–O–V bonds (ca. 900 cm^{-1}). The polymeric-to-isolated population ratio for V2 is lower than that for V5, as estimated from the relative intensities of the Raman bands near 900 and 1020 cm^{-1}. The TPR-Raman data for V11 are depicted in Fig. 4. All the bands related to $AlVO_4$ of V11 decrease quite simultaneously. It is difficult to evaluate the presence of surface vanadium oxide species on V11 since the Raman signal for $AlVO_4$ is several times more intense than that of surface vanadium oxide species.

3.2. H_2-TPR and kinetic modelling

Fig. 5 presents the TPR patterns of the catalysts V2, V5 and V11 collected at the heating rate of 6 °C/min. The H_2-TPR spectra of the samples V2 and V5 exhibit globally one clear maximum, whereas V11 has two predominant maxima. Fig. 6 depicts the TPR results of V5 with three different heating rates. Careful observation of the V5 spectra reveals a slight peak splitting after the rate maximum and a tailing of the signal on the high temperature side. The reduction process takes place in a wide temperature range. The temperatures of reduction rate maximum (T_{max}) for the first peak of the catalysts V11 and V5 coincide. The reduction rate maximum for the sample V2 occurs at 15 K

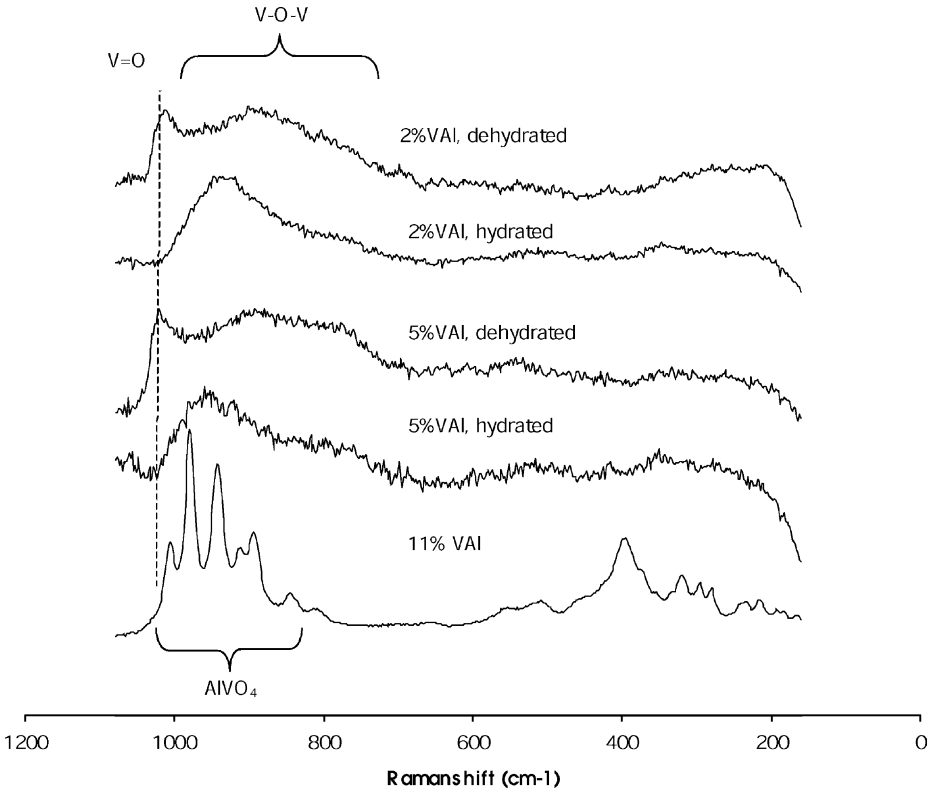

Fig. 3. Raman spectra of hydrated and dehydrated catalysts.

higher temperature. The second rate maxima of V11 appears at roughly 120 K after the first one. Table 1 collects the direct H_2-TPR results. The average oxidation states of vanadium were calculated according to the consumption of H_2 to 630 °C. The oxidation state of the vanadium was assumed to be +5 before reduction [16].

All H_2-TPR experiments were used for kinetic modelling of reduction. The total hydrogen consumption was scaled to unity in kinetic model fitting and the rate of hydrogen consumption was unequivocally related to the rate of reduction. Since hydrogen conversion was negligible during the TPR, the consumption of hydrogen was assumed not to affect the rate of reduction. Typical models [22] for the rate of conversion and combinations of them were tested by applying non-linear regression analysis to the TPR data of each catalyst with 3–4 heating rates. The random nucleation, nuclei growth model and shrinking core model were selected as potential model candidates. Also multiple reducible sites and multi-step models were taken into consideration. Model discrimination was based on the value of the object function (SSRs) and the quality of pointwise calculated residual plot.

The reduction of the catalyst V5 was focused first. Despite the apparent single-peak behaviour of the V5 thermogram, any attempted single reduction process could not satisfactorily describe the main reduction peak of V5. A very rough approximation of the main peak was accomplished using a random nucleation model. Total TPR pattern required altogether three sub-processes for a satisfactory fit and a non-biased residual plot. The best-fit to the TPR data of V5 was obtained with the a combination of a first-order model ($k_{ref} = (9.5 \pm 0.3) \times 10^{-2}\,s^{-1}$, $E = 100 \pm 2$ kJ/mol) and a two-dimensional nuclei growth model ($k_{ref} = (7.2 \pm 0.1) \times 10^{-2}\,s^{-1}$, $E = 90 \pm 2$ kJ/mol) for the main peak, and a first-order model for the process at the tail ($k_{ref} = (10.5 \pm 0.5) \times 10^{-3}\,s^{-1}$, $E = 74 \pm 3$ kJ/mol). All the reactions were modelled occur-

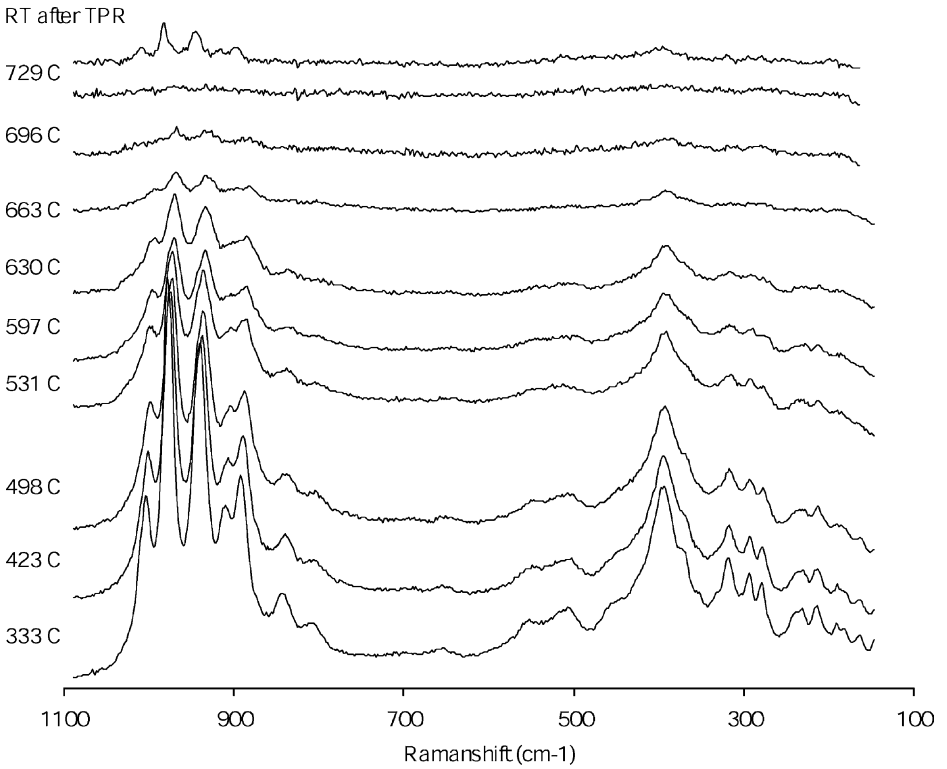

Fig. 4. Representative spectra of the TPR-Raman of the catalyst V11.

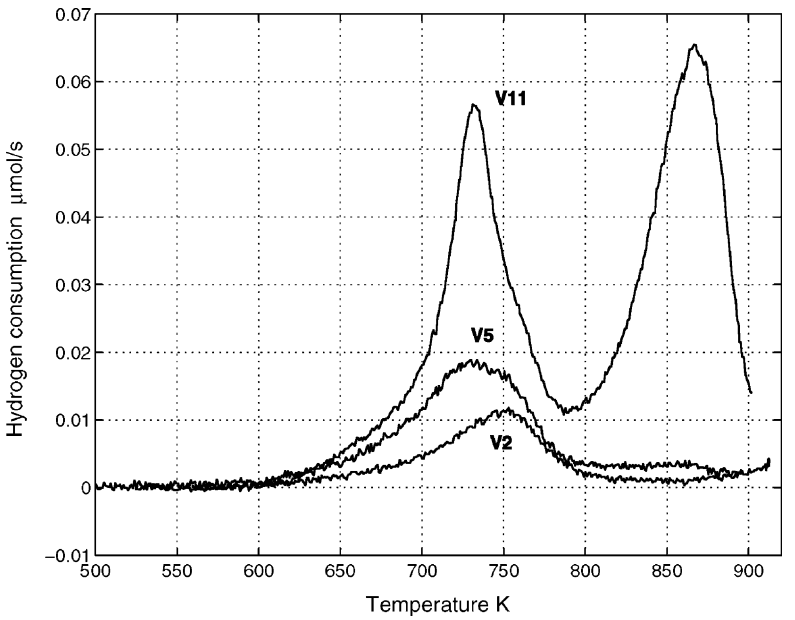

Fig. 5. H_2-TPR of the catalysts V2, V5 and V11 ($\beta = 6\,^{\circ}$C/min, $x_{H_2} = 10.7\%$ and $F = 30\,\mathrm{cm^3_{NTP}/min}$).

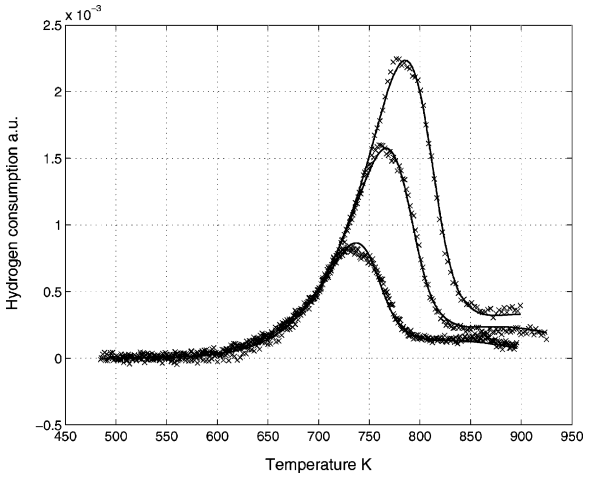

Fig. 6. H_2-TPR data (x) of the catalyst V5 (β = 6, 11 and 17 °C/min, x_{H_2} = 10.7% and $F = 30\,cm^3_{NTP}/min$) and the best-fit model solution (—).

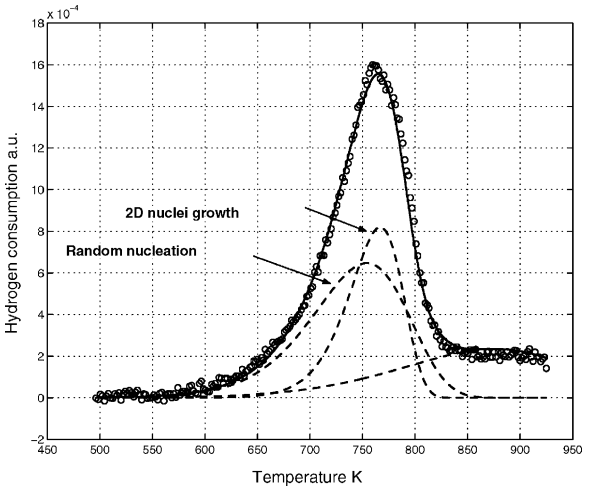

Fig. 7. H_2-TPR data (○) of the catalyst V5 and the best-fit model solution (- - -) with the subprocesses.

ring parallel and independent of each other. The contributions of these three processes to the total hydrogen consumption were 43, 30 and 27%, respectively. It is noteworthy, for example, that a model combining two random nucleation processes for the main peak could not perform nearly as well as the best-fit model. The best-fit model solution and the experimental data are presented in Fig. 6. Fig. 7 illustrates the best-fit model solution with the sub-processes.

The TPR data of V11 had two prominent rate maxima. Both reduction processes were characterised by a very steep acceleration period and a sharp maximum. These characteristics encouraged introducing models based on nuclei growth mechanism. The first peak was indeed best described by two-dimensional nuclei growth model with parameters $k_{ref} = (6.3 \pm 0.1) \times 10^{-2}\,s^{-1}$ and $E = 87 \pm 2$ kJ/mol. Same model type seemed also to be the best one for the latter peak with parameters $k_{ref} = (3.9 \pm 0.2) \times 10^{-3}\,s^{-1}$ and $E = 119 \pm 2$ kJ/mol. The latter process did not complete during the linear temperature program, except for the lowest heating rate and for that reason the modelling of the latter peak remains somewhat inconclusive. Any added third process to the total scheme did not result in a better fit. Generally, one would expect that, the three-dimensional nuclei growth or the shrinking core model would better describe actual bulk reduction processes. However, this was not the case with our experimental data.

Despite the low quality of the TPR data of the sample V2, kinetic modelling was attempted. V2 data set showed qualitative features characteristic for the first-order kinetic behaviour. Random nucleation model with parameters $k_{ref} = (6.8 \pm 0.2) \times 10^{-2}\,s^{-1}$ and $E = 146 \pm 3$ kJ/mol was indeed the only one-site model to roughly fit the experimental data. A model

Table 1
H_2-TPR results for the catalysts[a]

Vanadium content		Total H_2 consumption (μmol/g_{cat})	H_2/V (mol/mol)	AOS of V	T_{max}, K ($\beta = 6$ °C/min, x_{H_2} = 10.7%)
V (wt.%)	Atoms/nm^2				
2.0	1.4	195	0.50	+4.0	753
5.2	3.7	640	0.62	+3.7	729
11.4	9.4	1610	0.72	+3.6	731, 867

[a] Average oxidation state of V after the reduction to 630 °C.

combining two random nucleation processes was able to describe the results only slightly better and thus the possible second process was practically unidentifiable.

4. Discussion

The obtained kinetic results combined to the characterisation results allow further insight about the reduction behaviour of the studied catalysts. The redox properties are evidently dependent on the vanadium loading. The species on V2 and crystalline species on V11 are the least reducible. Part of the species on V5 reduces possibly in similar manner to the ones on V11. The TPR data of V2 and V5 suggests that different kinds of vanadium oxide surface species are relatively equal in the interaction with hydrogen. This complicates the deconvolution of TPR patterns into physically meaningful subprocesses. The kinetic modelling results imply, however, that there exist various reducible sites and reduction mechanisms.

Kinetic modelling was focused on the reduction of V5 catalyst because its vanadium content was below so-called monolayer vanadium oxide catalyst (8 V atoms per nm^2 on alumina support [23]). The whole TPR data of the catalyst V5 was deconvoluted into three reduction processes. The main peak was best described by a combination of a first-order (random nucleation) model and a two-dimensional nuclei growth model. The random nucleation mechanism was responsible for the onset of the main TPR peak and it is possibly related to the homogeneous reduction of surface vanadium oxide either isolated monomeric vanadium oxide species or predominantly oligomeric vanadium oxide species of moderate size. The two-dimensional nuclei growth is related to topochemical reduction of two-dimensional surface polymeric vanadium oxide species. The two-dimensional nuclei growth model states that the reduction is initiated somewhere in the surface oxide layer and it subsequently proceeds to the surroundings of the starting points. The domains of reduced vanadium grow outwards until they reach the boundaries of the reducible material or the boundaries of each other. The precondition for the physical feasibility of the two-dimensional nuclei growth reduction mechanism is that vanadium oxide species interact with the surrounding vanadium oxide species and thus form a contiguous overlayer. The reactivity is higher at the boundary of the reduced and the non-reduced phase than in the middle of non-reduced phase.

It has been observed that under reducing conditions, silica-supported vanadium oxide species undergo structural rearrangements that may lead to their aggregation into bulk V_2O_5, if vanadium oxide coverage is near the dispersion limit [8]. Thus, the reduction of V5 might induce structural transformation of surface vanadium oxide species as well, even though it does not lead to the formation of bulk V_2O_5 according to the TPR-Raman results. The interaction of vanadium oxide with alumina support is stronger than with silica support and the mobility of surface vanadium oxide species on alumina is consequently lower.

The special features of TPR pattern for V5 indicate that the structure of the catalyst is more complicated than a monolayer of vanadium oxide. Namely, the slight tailing on the high temperature side might infer to the reduction of bulk-like species, which do not exhibit sufficient crystallinity to be detected by our techniques. This tailing in the TPR profiles could reflect an incipient rearrangement of partially reduced surface vanadium oxide species, which might eventually lead to the formation of crystalline vanadium oxide, as in [8]. The second reduction process of V11 sample appears also at same temperatures as the tailing process of V5 (Fig. 5). Bulk-like species are evidently less reducible than two-dimensional surface vanadium species, which may be due to the diffusion of subsurface oxygen to the surface. In the kinetic modelling this high temperature hydrogen consumption was accounted for by introducing a first-order model to correct for the signal tailing. The obtained parameters for this process are of limited significance. Neither Raman spectroscopic nor XRD results give indication on the nature of these species.

Nuclei growth models had been proposed earlier for the reduction of supported vanadium oxide by Tarfaoui [24] and by Bosch and Sinot [25]. Tarfaoui [24] investigated thoroughly TPR of a monolayer vanadium oxide on alumina by the Kissinger and the Friedman analysis and kinetic model fitting. The Friedman plots of that work suggested a convoluted reduction process, but the best kinetic model was still one-site Avrami two-dimensional nucleation model with the activation energy of 108 kJ/mol. Bosch and Sinot [25] reported applicability of the nuclei growth model for the

reduction kinetics of vanadium oxide on titania monolayer catalyst. They obtained the activation energy of 60 kJ/mol. However, their modification of Avrami's nucleation model leaves some open questions. Our results suggest that nuclei growth plays a role in the reduction of V5 sample. It should be noted that a kinetic model combining two random nucleation processes did not perform nearly as well in describing the main peak of V5. However, nuclei growth model contributes less than a half of the hydrogen consumption of the main peak and it cannot alone explain the pre-edge of the V5 thermograms. The reason for this is believed to be the submonolayer content of vanadia on the sample V5. The vanadia does not form sufficiently contiguous overlayer. The reduction reaction on smaller domains of vanadium oxide is not able to advance further and their reduction is thus better described by random nucleation model.

Despite the overlapping multiple peak TPR spectra, kinetic modelling managed to provide additional information regarding the reduction of V11. The first peak of V11 probably involves the reduction of similar species to the ones present in V5 or some other kind of surface vanadium oxide species, perhaps an incipient $AlVO_4$ phase. The latter peak is related to the reduction of bulk-like vanadium compounds that can be present on high loaded samples. Indeed, the XRD results relate this latter reduction peak to the reduction of mixed oxide $AlVO_4$. The Raman results also reveal the presence of $AlVO_4$ in the fresh sample. The first peak of V11 possibly corresponds to the reduction of amorphous two-dimensional highly polymeric surface species (not visible in XRD and possibly hidden in Raman due to overwhelming intensity of partly overlapping $AlVO_4$ band in the 777–1070 cm^{-1} window), and it is clearly best described by two-dimensional nuclei growth kinetic model. The closeness of the activation energy values of nuclei growth for V5 (90 kJ/mol) and for the first peak of V11 (87 kJ/mol) suggests that reduction kinetics and energetics of these species are similar. On the other hand, the hydrogen consumption in the first TPR peak of V11 is high to be related to surface dispersed vanadium oxide. If the first TPR peak of V11 corresponds to some kind of incipient amorphous $AlVO_4$, the chemical nature of the reducible sites in this phase is closer to that in surface dispersed vanadium oxide than that in crystalline $AlVO_4$. The sample V11 contains probably larger contiguous arrays of highly polymerised vanadium oxide and this mode of organisation enables reduction predominantly by nuclei growth. The fact, that the latter peak of V11 also exhibited two-dimensional nuclei growth characteristics was unexpected. Since the second process does not complete by the end temperature the findings regarding the kinetic model remain uncertain.

A reduction process with random nucleation dynamics was identified based on the experimental data of the catalyst V2. The random nucleation, i.e. first-order decay model is acceptable for the reduction of V2, since the catalyst represents clearly a submonolayer vanadium content catalyst. The separation of the species from one another prevents the nuclei growth reduction mechanism that seems to be present on higher loaded samples. There is also no diffusion resistance in the oxygen removal from these vanadium species. The description given by the model was not perfect, however, but a secondary reduction process could not be properly identified. Raman results suggest that in addition to surface monovanadates there do exist surface polyvanadates. The presence of surface polymeric vanadium oxide is consistent with the presence of a broad Raman band near 900 cm^{-1} for catalyst V2, characteristic of the V–O–V bond stretching mode. The reduction kinetic results imply that either these polyvanadates are in minority among the vanadium oxide species or their reduction resembles closely that of monovanadates. Bulushev et al. [26] also found that first-order kinetic model described the reduction of a submonolayer vanadium oxide catalyst. The kinetic parameters cannot be compared because their catalyst was supported on TiO_2.

5. Conclusions

Alumina-supported vanadium oxide catalysts with the vanadium contents of 2, 5 and 11 wt.% were prepared by incipient wetness impregnation and characterised by XRD, TPR-Raman spectroscopy and H_2-TPR. The catalysts with the low vanadium contents contained surface dispersed vanadium oxide species, but the catalyst with the highest vanadium content contained also crystalline $AlVO_4$ according to XRD and Raman spectroscopic results. The presence of surface vanadium oxide species on V11 could not be ascertained by Raman spectroscopy due to the

intense Raman bands of $AlVO_4$. The reduction kinetics of vanadium oxide was modelled based on the hydrogen consumption during the TPR.

The reduction kinetics of catalyst with 2 wt.% V was best described by the random nucleation model. For the catalyst with 5 wt.% V, our kinetic modelling suggests that a part of vanadium species possibly reduces as a random nucleation process, but a topochemical reduction by nuclei growth also takes place. Both processes are related to surface vanadium oxide but possibly with different degree of interconnection to other vanadium oxide entities. The catalyst with 11 wt.% V reduces clearly in two separate processes. The first reduction peak is described by two-dimensional nuclei growth model and it must be related to amorphous surface vanadium oxide and the latter reduction peak is assigned to crystalline $AlVO_4$. Evidently, the vanadium loading has a pronounced effect on the structure of the catalyst and consequently to the reduction behaviour.

Acknowledgements

We thank Ms. Marja-Leena Saanto at Fortum Oil and Gas Oy for preparing the catalyst samples and Ms. Heidi Österholm at Fortum Oil and Gas Oy for the XRD analyses. CICYT Grant IN96-0053, Spain, partially funded the acquisition of the Raman spectrometer. Support from European Union COST Action D15 WG 0021-01 is acknowledged.

References

[1] T. Blasco, J.M. López Nieto, Appl. Catal. A 157 (1997) 117.
[2] E.A. Mamedov, V. Cortés Corberán, Appl. Catal. A 127 (1995) 1.
[3] F. Cavani, F. Trifirò, Catal. Today 51 (1999) 561.
[4] S. Albonetti, F. Cavani, F. Trifiró, Catal. Rev.-Sci. Eng. 38 (1996) 413.
[5] L.J. Alemany, L. Lietti, N. Ferlazzo, P. Forzatti, G. Busca, E. Giamello, F. Bregani, J. Catal. 155 (1995) 117.
[6] J. Haber, in: G. Ertl, H. Knözinger, J. Weitkamp (Eds.), Handbook of Heterogeneous Catalysis, vol. 5, VCH, Weinheim, 1997, p. 2253.
[7] X. Gao, M.A. Bañares, I.E. Wachs, J. Catal. 188 (2) (1999) 325.
[8] M.A. Bañares, J.H. Cardoso, F. Agulló-Rueda, J.M. Correa-Bueno, J.L.G. Fierro, Catal. Lett. 64 (2000) 191.
[9] J.M. López Nieto, J. Soler, P. Concepción, J. Herguido, M. Menéndez, J.J. Santamaria, Catalysis 185 (1999) 324.
[10] G. Busca, E. Finocchio, G. Ramis, Ricchiardi, Catal. Today 32 (1996) 133.
[11] M. Bañares, Catal. Today 51 (1999) 319.
[12] H. Bosch, B.J. Kip, J.G. Van Ommen, P.J. Gellings, J. Chem. Soc., Faraday Trans. 80 (1984) 2479.
[13] D. Ballivet-Tkatchenko, G.J. Delahay, J. Therm. Anal. 41 (1994) 1141.
[14] J. Sloczynski, J. Appl. Catal. A 146 (1996) 401.
[15] M.A. Centeno, J.J. Benitez, P. Malet, I. Carriozosa, J.A. Odriozola, Appl. Spectrosc. 51 (1997) 416.
[16] M.E. Harlin, V.M. Niemi, A.O.I. Krause, J. Catal. 195 (2000) 67.
[17] M.E. Harlin, V.M. Niemi, A.O.I. Krause, B.M. Weckhuysen, J. Catal. 203 (2001) 242.
[18] J.M. Kanervo, A.O.I. Krause, J. Phys. Chem. B 105 (2001) 9778.
[19] J.M. Kanervo, A.O.I. Krause, J. Catal. 207 (2002) 57.
[20] P. Malet, A. Caballero, J. Chem. Soc., Faraday Trans. 84 (1988) 2369.
[21] H.S. Fogler, Elements of Chemical Reaction Engineering, 3rd ed., Prentice-Hall, Englewood Cliffs, NJ, 1999, p. 758.
[22] J.A. Moulijn, P.W.N.M. van Leeuwen, R.A. van Santen, Catalysis—An Integrated Approach to Homogenous, Heterogeneous and Industrial Catalysis, Netherlands Institute for Catalyst Research, Elsevier, Amsterdam, 1993, p. 411.
[23] I.E. Wachs, B.M. Weckhuysen, Appl. Catal. A 157 (1997) 67.
[24] A. Tarfaoui, Ph.D. Thesis, Delft University of Technology, The Netherlands, 1996.
[25] H. Bosch, P.J. Sinot, J. Chem. Soc., Faraday Trans. I 85 (1989) 1425.
[26] D.A. Bulushev, L. Kiwi-Minsker, F. Rainone, A. Renken, J. Catal. 205 (2002) 115.